THE JOURNAL OF PHYSICAL CHEMISTRY Letters

Letter

pubs.acs.org/JPCL

Influence of the Carotenoid Composition on the Conformational Dynamics of Photosynthetic Light-Harvesting Complexes

Marijonas Tutkus,[†] Jevgenij Chmeliov,[†,‡] Danielis Rutkauskas,[†] Alexander V. Ruban,[§] and Leonas Valkunas*[,†,‡]

[†]Department of Molecular Compound Physics, Center for Physical Sciences and Technology, Saulėtekio Avenue 3, LT-10257 Vilnius, Lithuania

[‡]Institute of Chemical Physics, Faculty of Physics, Vilnius University, Saulėtekio Avenue 9, LT-10222 Vilnius, Lithuania

[§]The School of Biological and Chemical Sciences, Queen Mary, University of London, Mile End Road, London E1 4NS, United Kingdom

Supporting Information

ABSTRACT: Nonphotochemical quenching (NPQ) is the major self-regulatory mechanism of green plant, performed on a molecular level to protect them from an overexcitation during the direct sunlight. It is believed that NPQ becomes available due to conformational dynamics of the light-harvesting photosynthetic complexes and involves a direct participation of carotenoids. In this work, we perform a single-molecule microscopy on major light-harvesting complexes (LHCII) from different *Arabidopsis thaliana* mutants exhibiting various carotenoid composition. We show how the distinct carotenoids affect the dynamics of the conformational switching between multiple coexisting light-emitting states of LHCII and demonstrate that properties of the quenched conformation are not influenced by the particular carotenoids available in LHCII. We also discuss the possible origin of different conformational states and relate them to the fluorescence decay kinetics observed during the bulk measurements.

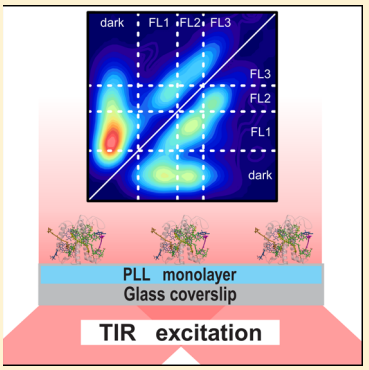

The importance of photosynthesis and its role in the Earth's ecosystem is difficult to overestimate: it is the key physiological process performed by green plants, algae, and some bacteria that is responsible for the initial step of biomass production and refilling the atmosphere with oxygen. To efficiently perform this task, distinct photosynthetic organisms have developed various photosynthetic apparatuses different in structure but similar in design. Their "photosynthetic factories" comprise a huge number of pigment molecules, usually bound to a protein scaffold and distributed over a photosynthetic membrane.[1,2] Both the mutual arrangement of the pigments and their spectroscopic properties have been carefully adjusted by Nature to optimize an overall efficiency of the photosynthetic light-harvesting antenna: up to 99% of the absorbed photons are successfully utilized during the later stages of photosynthesis.[1−4] While such an efficiency helps photosynthetic organisms to survive and to function at very low illumination conditions (like underwater environment or deep continuous shadow), bright sunlight might result in an overexcitation of the light-harvesting antenna and lead to the formation of highly reactive singlet oxygen species. In order to avoid any possible photodamage, over ages of evolution, plants have developed various self-regulatory mechanisms. The most efficient one, operating on a molecular level and dissipating the excess excitation as heat, reversibly forms and relaxes within several seconds to minutes and is commonly known as an energy-dependent (qE) part of nonphotochemical quenching (NPQ).[5] Many studies aiming to reveal the molecular origin of NPQ have been carried out over the last two decades (see, e.g., the recent review by Ruban et al.[5]), but the final answer is still to be found, although more evidence for the direct involvement of the carotenoid (Car) molecules appears.[6−11]

The larger part of the photosynthetic antenna of plants is built from the trimeric major light-harvesting complexes (LHCIIs) that bind more than 50% of all the terrestrial chlorophyll (Chl) molecules.[1] These complexes, however, are known not only for the efficient light harvesting, but also for participation in various regulatory processes. First, depending on the spectral composition of the incoming light, LHCII trimers can diffuse through the thylakoid membrane between different photosynthetic units to optimize their relative absorption cross sections.[12] Besides that, LHCII complexes participate in the dynamic variation of the antenna size during high light conditions[13] and are also supposed to be the most probable location for the NPQ traps.[5]

The crystal structure of the LHCII complexes, known with a sub-3 Å resolution,[14] reveals the mutual arrangement of 8 Chl *a* and 6 Chl *b* molecules as well as 4 Car pigments: 2 luteins (Lut), 1 neoxanthin (Neo), and 1 xanthophyll cycle carotenoid (either violaxanthin (Vio) or zeaxanthin (Zea)) per each

Received: October 5, 2017
Accepted: November 15, 2017
Published: November 15, 2017

DOI: 10.1021/acs.jpclett.7b02634
J. Phys. Chem. Lett. XXXX, XXX, XXX−XXX

monomeric subunit (see Figure 1a for schematic view). Neo, the most polar and asymmetric of these Cars, is found on a Chl

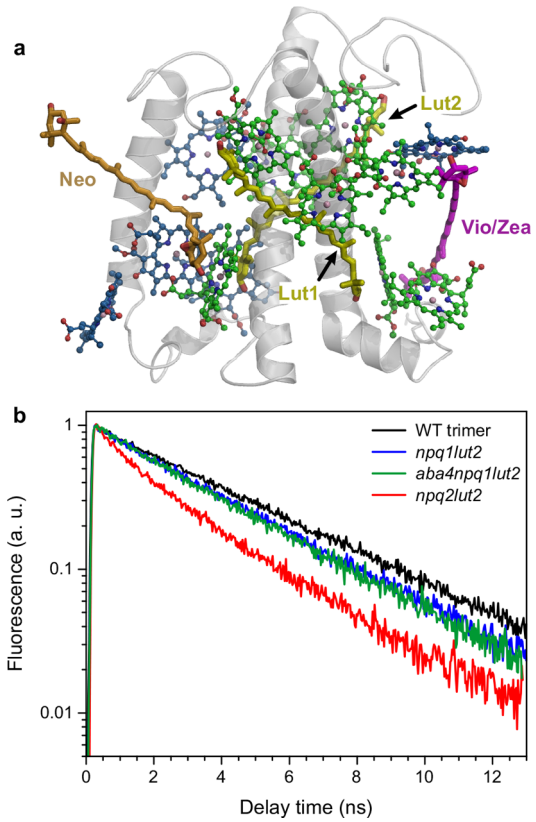

Figure 1. (a) Crystal structure of LHCII monomer and carotenoid binding sites (Lut1, Lut2, Vio, and Neo/Zea).[14] Chls *a* are indicated with green, Chls *b* with blue, both luteins with dark yellow, Vio with magenta, Neo with orange, and protein helices with gray. (b) Fluorescence decay kinetics in the detergent-solubilized LHCII complexes from WT *Arabidopsis* as well as *npq1lut2* (containing Vio and Neo carotenoids), *aba4 npq1lut2* (binding Vio as the only Car), and *npq2lut2* (binding Zea as the only Car) mutants, measured at 273 K.

b-rich peripheral side of LHCII. The xanthophyll cycle Car is located at the interface between the two monomeric subunits of the LHCII trimer. Exposure to high light results in a reversible de-epoxidation of Vio into Zea, which promotes the clustering of the LHCII complexes, leading to a more efficient excitation energy quenching.[5] Finally, the remaining two Cars, luteins, are arranged in a cross pattern and assist in holding the LHCII complex together.[14] This Car is also known to be responsible for the trimerization of LHCII;[15] therefore lutein-deficient plants are able to form only monomeric light-harvesting complexes.[16] Moreover, one of these luteins, namely Lut1, is located close to the so-called chlorophyll terminal emitter the cluster of 3 Chl molecules of the lowest site energies, which makes it a favorable candidate to govern NPQ.[8]

To study the role of each carotenoid in light harvesting and self-regulation, the targeted mutagenesis of various photosynthetic antenna complexes has been widely applied.[6,16−22] By blocking the specific paths of Car biosynthesis, LHCIIs with different xanthophyll composition can be obtained, causing specific structural variations that affect the overall excitation energy dynamics in the light-harvesting antenna.[16] In this work, we utilize the methods of single molecule (SM) microscopy to examine fluorescence (FL) intensity fluctuations in single monomeric LHCII subunits from the lutein-deficient *Arabidopsis thaliana* mutants. In particular, we study the double mutant *npq1lut2*,[17] which is incapable of synthesizing either Zea or Lut and therefore accumulates only Vio and Neo, and the triple mutants *aba4npq1lut2*[20] and *npq2lut2*,[23] accumulating Vio and Zea, respectively, as the only carotenoid. The Car composition of these mutants is also summarized in Table 1. For reference, isolated trimeric LHCII complexes from unaffected wild-type (WT) *Arabidopsis thaliana* were also analyzed.

Table 1. Carotenoid Composition in the LHCII Samples Studied in This Work

sample	bound carotenoids
WT	Lut, Vio, and Neo
npq1lut2	Vio and Neo
aba4npq1lut2	Vio
npq2lut2	Zea

Fluorescence decay kinetics in the mentioned bulk solubilized LHCII samples, measured with a streak-camera at 273 K temperature, are shown in Figure 1b. Those in all mutants clearly demonstrate somewhat faster decay behavior compared to the WT species. Thus, replacement of the lutein pigments by the xanthophyll cycle carotenoid (either Vio or Zea) possibly opens some additional weak channel for excitation quenching, not available in wild-type LHCIIs. Since Neo is located in the Chl *b*-rich region of the LHCII monomer (cf. Figure 1a), its replacement by the Vio pigment in the *aba4npq1lut2* mutant does not influence the mean relaxation rate of the Chls *a* (mean excitation lifetimes in the *npq1lut2* and *aba4npq1lut2* mutants are 3.3 and 3.2 ns, respectively). Meanwhile, *npq2lut2* mutant, incapable of synthesizing any carotenoid except Zea, shows huge qualitative difference in the fluorescence decay kinetics, clearly exhibiting a strongly biexponential decay behavior contrary to all three of the other samples, demonstrating almost single-exponential decay (see Table S1 for lifetimes and their amplitudes). The appearance of the additional fast decay component of 0.8 ns strongly suggests that a new conformational state of the protein scaffold, notably enhancing excitation quenching, becomes available in this mutant. To perform further analysis of the intrinsic conformational states and their dynamics, we continued with SM microscopy measurements of single LHCII complexes, immobilized on the PLL modified glass coverslips in detergent micelles.

For our measurements, we used total internal reflection (TIR) objective-based microscope setup equipped with the EM-CCD camera working at 30 ms integration time and 635 nm laser excitation.[24] This method allowed us to subject LHCII complexes to the continuous <1 W/cm^2 illumination, which is considerably lower than typical intensities utilized in confocal microscopy,[25−30] thus we completely avoid any singlet singlet and singlet triplet annihilation (taking into account the absorption cross-section of an LHCII trimer of $\sigma = 1.4 \times 10^{-15}$ cm^2,[31] the probability of simultaneous generation of two singlet excited states is negligible, and the probability of accumulating a triplet state[32] is less than 1%). Nevertheless, such low illumination conditions are quite close to the mean natural solar radiation hitting the Earth surface during a sunny day. In addition, by using TIR microscopy, we excite only a

DOI: 10.1021/acs.jpclett.7b02634
J. Phys. Chem. Lett. XXXX, XXX, XXX−XXX

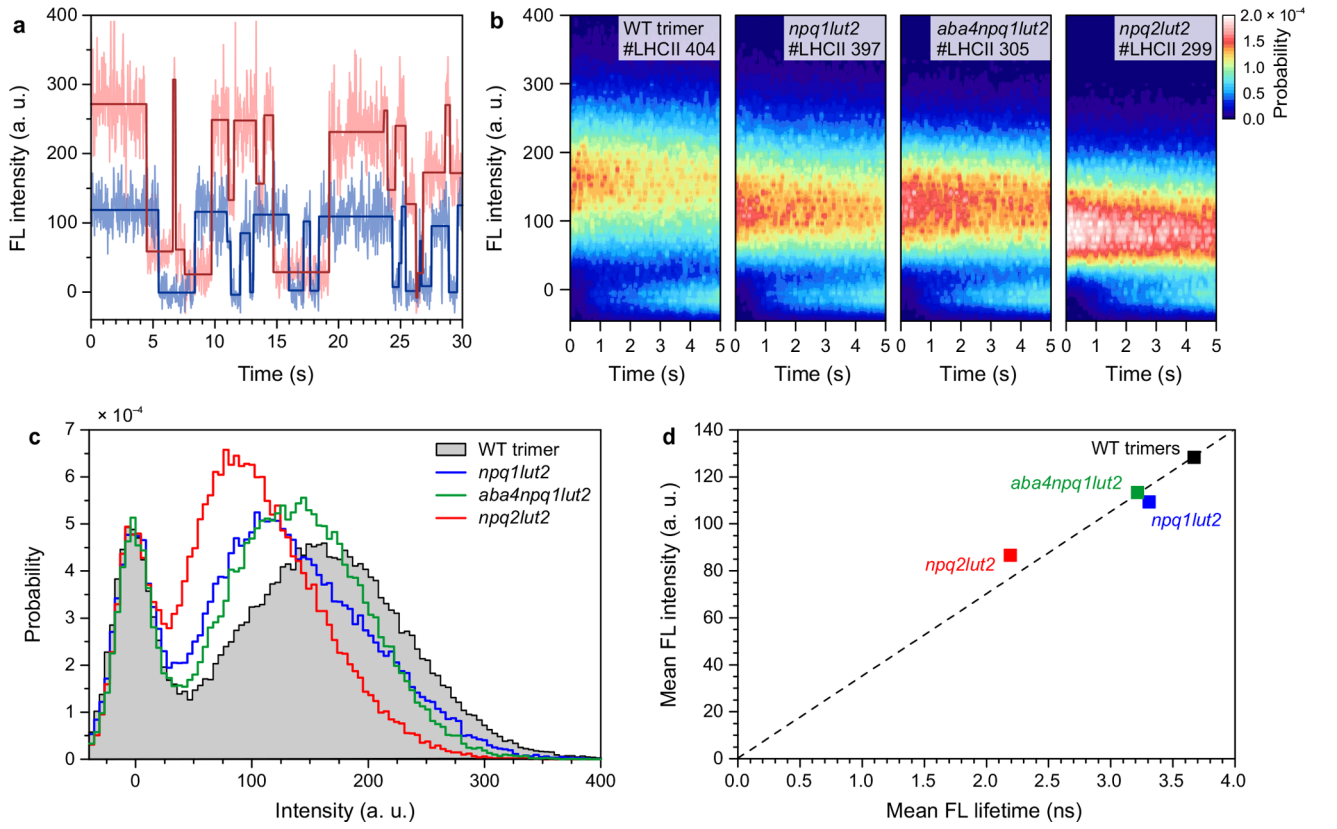

Figure 2. Fluorescence measurements in single LHCII complexes. (a) Two representative time traces of the fluorescence intensity fluctuations, measured for two different wild-type LHCII trimers (0 FL intensity level is set as the mean intensity value of the dark state). Dark step lines represent resolved intensity levels. (b) Color-coded distribution of the fluorescence intensities at different time delays, measured in WT LHCII trimers and LHCII monomers from *npq1lut2*, *aba4npq1lut2*, and *npq2lut2* mutants. These distributions were acquired by collecting fluorescence time traces similar to those shown in panel (a), obtained from 300−400 (the exact number is indicated in each case) single LHCII complexes. (c) Total distribution of the resolved fluorescence intensity levels in four different LHCII samples shown in panel b. These distributions are normalized to unit area. (d) Correlation between the mean fluorescence intensities in the SM spectroscopy measurements, obtained from the FL intensity distributions shown in panel c, and the mean fluorescence lifetimes in the mentioned samples, obtained from the FL decay kinetics in the solubilized LHCIIs shown in Figure 1b.

small distance (~15 nm) perpendicular to the glass coverslip, which gives negligible background signal and enables much better signal-to-noise ratio than confocal microscopy. Since the signal from all the LHCII complexes is monitored mostly simultaneously, the whole measurement takes less time and guarantees that all of the measured complexes were exposed to very similar conditions. And finally, TIR setup is equipped with an EM-CCD camera, which has very high detection sensitivity (quantum efficiency about 80% in the region of LHCII emission), low noise, and excellent detection stability.

The acquired fluorescence signal coming from the single LHCII complexes exhibited a well-known blinking behavior,[25−30] when FL intensity switches quickly and reversibly between several stable emission levels as a result of the conformational variations of the protein scaffold[33] (see Figure 2a for the FL intensity fluctuations in two distinct wild-type LHCII trimers). Such time traces of the fluorescence intensity fluctuations were collected for 404 distinct WT LHCII trimers, and the time-dependent distribution of all the obtained emission levels is shown in the left panel of Figure 2b as a color-coded two-dimensional fluorescence map. This map reveals that the intensities of the highly emitting states are broadly distributed around the intensity level of ~160 a. u., whereas the second much narrower peak at ~0 a. u. represents nonfluorescing, or quenched, LHCII complexes (if the switching to this state was reversible) or, alternatively, the complexes being completely bleached (when the switching to the dark state was irreversible). Since only those single LHCII complexes initially being in their light-emitting conformational state were detected, there was a relatively small number of dark states detected during the first second. Later on, more complexes reversibly switch to the dark state, thus the zero-intensity level becomes populated more often. After ~25 s of continuous illumination, the majority of the detected complexes were bleached (cf. Figure S1). Only the part of the FL time trace prior to photobleaching of each LHCII complex was considered in any further analysis.

In order to compare the statistical properties of the fluorescence blinking in different LHCII samples, analogous measurements were also performed for LHCII monomers from three lutein-deficient mutants mentioned above. The obtained results are summarized in Figure 2b and qualitatively resemble those collected from the WT LHCII trimers. The most apparent difference is the decrease of the mean FL intensity of the fluorescing state in all the mutants compared to that in the WT samples. This difference becomes even clearer in Figure 2c, where the overall distribution of the resolved emission levels is demonstrated. Interestingly, FL intensity in the LHCII monomers from the mutants does not exhibit a 3-fold drop compared to the wild-type LHCII trimers: while in the wild-

DOI: 10.1021/acs.jpclett.7b02634
J. Phys. Chem. Lett. XXXX, XXX, XXX−XXX

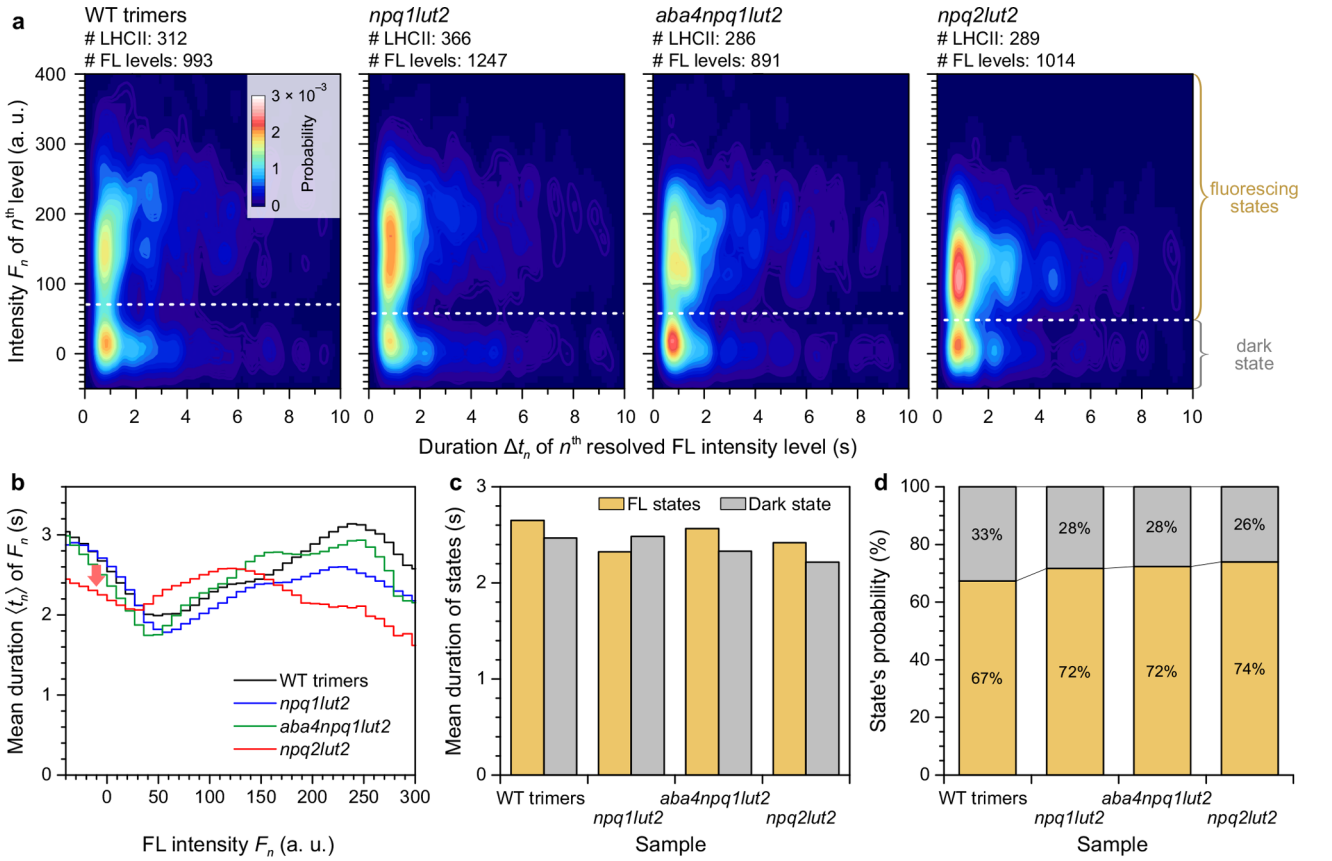

Figure 3. Correlation between the fluorescence intensity level (vertical axis) and the duration of detected states (horizontal axis). (a) Color-coded correlation maps, obtained for wild-type LHCII trimers as well as monomeric LHCIIs from the *npq1lut2*, *aba4npq1lut2*, and *npq2lut2* mutants. The number of LHCII complexes analyzed and the number of the resolved FL intensity levels is indicated separately in each case. The assignment of the distinct FL intensity levels to the dark and fluorescing states is indicated with horizontal white dashed lines. (b) Mean durations of various FL intensity levels in the single LHCII complexes from different samples, obtained from the correlation maps in panel a by averaging them over horizontal axis. Red arrow indicates a notable drop in the mean duration of the quenched state in the *npq2lut2* mutant. (c) Overall mean duration of the fluorescing and dark states of single LHCII complexes from various samples. (d) The relative probabilities the dark and fluorescing conformational states of various LHCII samples, obtained by integrating correlation maps in panel a over both vertical and horizontal axes within the domains separated by the white dashed lines.

type LHCII complexes the emission intensities of the highly fluorescing states are distributed around 160 a.u., the corresponding peak intensity dropped by ∼ one-quarter in the *npq1lut2* and *aba4npq1lut2* mutants (115 and 130 a.u., respectively). This indicates that, under our illumination conditions, the probability to absorb three photons per trimer while all its monomeric subunits are in the high-emitting state, might be rather low (see also Methods), although the possibility for trimeric and monomeric complexes to experience slightly different environments (e.g., they can be differently orientated during their immobilization on the PLL glass coverslip) also cannot be disregarded.

Distributions of FL intensities in both these mutants are very similar, again demonstrating that the replacement of the Neo with Vio in the latter one does not significantly change the overall excitation dynamics in LHCII. Meanwhile, in the LHCII monomers from npq2lut2 mutant, the drop in observed FL intensities was even more pronounced and exceeded 45% in these complexes, and the dominating fluorescence intensity decreased down to 85 a.u. In all the mutants, not only the maximum position of the band of the FL intensities of the strongly fluorescing states shifted toward lower intensities (comparing to the WT samples), but also the amplitude of this band (i.e., the number of occurrences of the corresponding FL levels) increased, while the width of this band decreased accordingly. Interestingly, neither the amplitude nor the width of the band corresponding to the nonfluorescing state exhibited any differences between different LHCII samples, suggesting the same physical origin of the dark state in all the cases. Indeed, distribution of intensities around this dark state was fitted with a Gaussian function, and its width within the fitting error was the same as for the bleached spot intensity distributions shown in Figure S1b (20.4 ± 1.9 and 20.6 ± 0.48 a.u., respectively). By taking an average of the whole distribution shown in Figure 2c, including the quenched and fluorescing states, the mean fluorescence intensities in different samples were calculated. These mean intensities correlate with the mean FL lifetimes observed during the bulk measurements, as shown in Figure 2d. Thus, we can conclude that the FL decay kinetics, reflecting excitation dynamics that occurs within the complex on a nanosecond time scale, is strongly related to the conformational dynamics of the complex as a single unit, taking place on a time scale from milliseconds to several seconds.

All four LHCII samples studied in this work exhibited a very broad distribution of the intensity levels of the fluorescing states. Thus, several distinct conformational states of the light-harvesting complexes, each corresponding to some specific

DOI: 10.1021/acs.jpclett.7b02634
J. Phys. Chem. Lett. XXXX, XXX, XXX−XXX

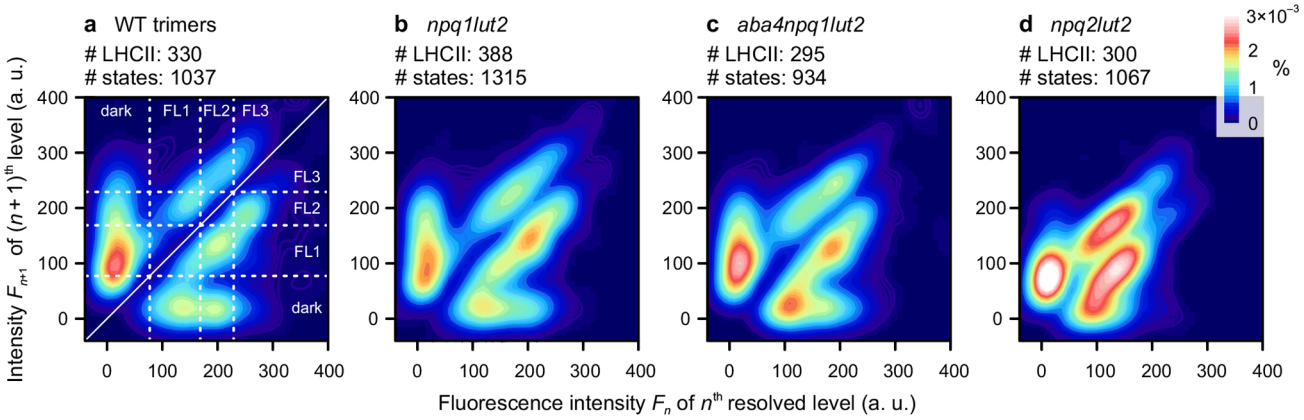

Figure 4. Transitions between different conformational states. (a) Two-dimensional transition density (TD) histogram plot for WT LHCII trimers, showing correlation between the mean intensity F_n of nth state (horizontal axis) and the mean intensity F_{n+1} of the following $(n + 1)$th state (vertical axis). The number of single LHCII trimers and the numbers of the resolved FL intensity levels are indicated at the top. The TD map is normalized to 1, and the color scale on the right indicates the probability of the corresponding transition $F_n \rightarrow F_{n+1}$. The observed cross-peaks correspond to the conformational switching between different states of LHCII, denoted as "dark", "FL1", "FL2" and "FL3" and separated with white dashed lines. LHCII monomers from the carotenoid mutants exhibit qualitatively similar correlation maps (b–d).

dominating fluorescence intensity, might coexist, as suggested previously.[25,29] To address this issue and to characterize possible conformational states, we have first evaluated the correlation between each resolved FL intensity level (F_n) and the time duration Δt_n that each LHCII complex was fluorescing with that particular intensity before a transition to another intensity level (F_{n+1}) occurred. The resulting two-dimensional histogram plots are shown in Figure 3a and demonstrate that the wide distribution of the intensities of the active (highly fluorescing) LHCII state in Figure 2c indeed has some intrinsic structure. For example, in the case of WT LHCII species, we can identify at least two distinct fluorescing states: one with the dominating fluorescence intensity around 150 a.u. and another around 230 a.u. The former state is more probable, but its duration on average is shorter. Qualitatively similar correlation pattern is obtained in LHCII mutants, although the dominating fluorescence intensities of the bright states are reduced.

Most of the detected FL intensity levels had a duration from several hundreds of milliseconds to ∼3 s, but longer-living states were also observed, in accordance with the well-known power-law distribution.[25,26] By averaging the correlation maps in Figure 3a over the horizontal axis, we obtain the mean durations $\langle \Delta t_n(F_n) \rangle$ of each resolved FL intensity level F_n, as shown in Figure 3b. While the mean duration of the FL intensity levels corresponding to the dark states (those around $F_n = 0$) in both *npq1lut2* and *aba4npq1lut2* mutants remain the same as in WT LHCII trimers, those in the *npq2lut2* exhibit a notable drop, as indicated by the red arrow in Figure 3b. On average, the dark conformation survives for 2.5 s in both WT trimers and *npq1lut2* mutants, its mean duration then decreased to 2.3 s in *aba4npq1lut2* and further dropped down to 2.2 s in the *npq2lut2* mutant (see Figure 3c). The description of the fluorescing states is complicated by the coexistence of multiple distinct conformations, thus only the mean duration of all these fluorescing conformational states can be reliably evaluated: while being 2.7 s in WT complexes, it decreases by 0.4, 0.1, and 0.3 s in *npq1lut2, aba4npq1lut2*, and *npq2lut2*, respectively. This results in slightly faster conformational dynamics in all the mutants compared to the wild-type LHCII trimers.

Finally, by integrating correlation maps shown in Figure 3a over both vertical and horizontal axes within the domains corresponding to the emitting and quenched states and separated by the white dashed lines, we can evaluate the overall probabilities of fluorescing and dark states, as demonstrated in Figure 3d. Counterintuitively, we see the stabilization of the fluorescing states (manifesting itself via 57% increase in probability) in all the mutants compared to the WT samples, despite the fact that the drop in the overall mean FL intensity and mean excitation lifetime, observed in the mutants and discussed above, would suggest an opposite effect. This could indicate that replacement of luteins by either Vio or Zea pigments results in more pronounced switching between different fluorescing conformational states and, accordingly, less frequent "visiting" of the quenched conformation.

To check this suggestion and to highlight the conformational dynamics between different conformational states of the LHCII complex, we have also calculated the correlation pattern of the intensities of two detected subsequent fluorescence levels (F_n and F_{n+1}). The resulting two-dimensional transition density (TD) histogram, describing probabilities of different transitions between the detected states (F_n) in the single-molecule fluorescence intensity traces from WT trimeric LHCIIs, is presented in Figure 4a. This TD map shows a complex landscape and further reveals the hidden structure of the main emission intensity band. Indeed, we can clearly distinguish several cross-peaks corresponding to various transitions between different conformational states: one such state is readily attributed to the aforementioned dark state (with FL intensity around 0 a.u.). However, we can also resolve at least three distinct fluorescing states corresponding to the fluorescence intensities of ∼100130 a.u., ∼200 a.u., and ∼250 a.u. (denoted in Figure 4a as FL1, FL2, and FL3, respectively). We can also note the asymmetry between different transition pathways: the most dominating transition corresponds to the conformational switch of the LHCII complex from the dark state into FL1 state, whereas the repopulation of the dark state occurs from both FL1 and FL2 states. Somewhat less probable transitions occur between FL2 and FL1 states as well as FL3 and FL2 states. Moreover, the elongation of the cross-peaks along the main diagonal rather reveals a high level of inhomogeneity of FL emission in different single LHCII complexes (see also FL time traces in Figure 2a, exhibiting

DOI: 10.1021/acs.jpclett.7b02634
J. Phys. Chem. Lett. XXXX, XXX, XXX−XXX

various FL intensities of the fluorescing states for distinct LHCIIs).

The corresponding TD maps, obtained for the lutein-deficient LHCII complexes, are shown in Figure 4b–d. Both *npq1lut2* and *aba4npq1lut2* mutants exhibit very similar transition pattern as the wild-type samples, except for the general drop in FL intensity. However, one can also note more frequent switching between distinct fluorescent states (represented by the increased amplitude of the cross-peaks at $F_n \approx 200$ and $F_{n+1} \approx 150$ a.u. and vice versa), thus supporting the suggestion made above. This effect is even more pronounced in the case of *npq2lut2*, shown in Figure 4d. In this mutant, only the emitting state corresponding to the *lowest* FL intensity is involved in the reversible transitions to/from the quenched state, whereas the conformational states attributed to higher FL intensity participate only in the switching to/from other emitting states.

Based on our measurements, several conclusions regarding conformational dynamics of LHCII complexes can be drawn. First of all, the mean fluorescence intensity, observed during the SM measurements and related to protein conformation dynamics, correlates with the time scale of fluorescence decay kinetics, representing excitation energy transfer and relaxation within the complex. Next, SM microscopy revealed a rather high level of heterogeneity of single LHCII complexes and quite complex conformational energy landscape. In particular, besides the quenched state, the coexistence of at least three distinct fluorescing conformational states, attributed to different FL intensity levels and experiencing strongly asymmetric switching between themselves, was revealed. Each such state might correspond to slightly different mutual arrangements of the pigment molecules within the LHCII complex and, as suggested earlier,[29] result in different time scales of excitation energy dynamics between the pigment molecules. Therefore, partially quenched, but still fluorescing state(s) might explain any nonexponentiality observed during the time-resolved fluorescence measurements.

We have also demonstrated that the replacement of the lutein pigments with either Vio or Zea, preventing the formation of tightly bound trimeric complexes, results in faster conformational dynamics compared to that observed in WT LHCII trimers. This explains why such monomeric pigment–protein complexes are more sensitive to a varying environment such as lumen protons, as was previously observed during the *in vitro* experiments.[34] Meanwhile, the fact that all the samples exhibited fluorescence blinking behavior and the observed properties of the dark conformational state were rather similar regardless of the carotenoid compositions reveals the identical nature of the quenching mechanism in all these LHCII complexes. Our observations suggest that not a particular carotenoid but rather a carotenoid that is bound to a specific binding locus acts as quenchers. Hence, the variability of LHCII carotenoid types is less critical than their environment. This result indirectly supports the model of incoherent excitation energy transfer from Chl molecule to the optically dark short-lived S_1 state of the available carotenoid.[8] Indeed, the coherent mixing of the Car and Chl excitonic states or, alternatively, the formation of the Car–Chl charge-transfer state would be very sensitive to the exact position of the Car S_1 energy level (with respect to the site energies of the nearby chlorophylls) and therefore would lead to different results in different samples. On the other hand, very broad density-of-states distribution of the Car S_1 transition results in very weak effect of both the Car S_1 site energy and small variations in the ChlCar couplings (expected to take place in our different samples with various carotenoid composition) on the rate of the incoherent Chl → Car excitation transfer.[35,36]

Nevertheless, the carotenoid composition does have some effect on the conformational switching of the LHCII complex between different emitting states. That is not surprising since carotenoids are essential structural elements of the light-harvesting complexes and, as such, they can affect the overall structure that, in its turn, influences the blinking behavior. However, transition density patterns, shown in Figure 4, reveal that the replacement of the luteins with Vio in both *npq1lut2* and *aba4npq1lut2* mutants results in very subtle structural variations that do not change the overall conformational dynamics of the LHCII monomer, but makes switching between the strongly and moderately fluorescing states more probable than in the WT samples. As a result, we observe somewhat smaller mean fluorescence intensity (Figure 2c) and slightly faster excitation decay kinetics (Figure 1b). Very similar results, obtained for both these mutants, also confirm that the Neo binding site in the Chl *b*-rich peripheral side participates neither in fluorescence quenching nor in the conformational dynamics of the pigment protein complex as a whole. On the other hand, the *npq2lut2* LHCII monomers, containing Zea as the only carotenoid, demonstrated even more pronounced switching between fluorescing and partially quenched states, which is in line with the observed nonexponentiality in fluorescence decay kinetics. The qualitative differences, observed for this mutant both in the bulk measurements (see Figure 1b) and by means of single-molecule microscopy (see Figures 3b and 4d), suggest that (at lest in this mutant) the mentioned partially quenching state cannot be simply the result of very fast switching between the fully quenched and fluorescing conformations, occurring within the binning time. Rather, some additional factors should be involved. The physical origin of this partially quenched conformational state could be related to the formation of Chl–Zea charge transfer state; the signatures of the presence of a Zea^+ radical cation were indeed observed earlier in the Zea-enriched photosynthetic antenna.[6,21] All these properties again demonstrate very flexible and highly adaptable self-regulation of plants, in general capable to dissipate the excess excitation energy using any carotenoids available and, if needed, also being prone to further fine-tuning by utilizing xanthophyll cycle to produce Zea and the corresponding partially quenched conformational state of the protein scaffold.

METHODS

Sample Preparation. Unstacked thylakoids were prepared from 100 g of dark-adapted *Arabidopsis thaliana* leaves with the midrib removed. Leaves were homogenized in 300 mL of icy grinding medium (0.33 Msorbitol, 10 mM Na4P2O7·H2O and 130 mg D-iso-ascorbate; pH 6.5) and the homogenate filtered through a bilayer of muslin cloth, followed by a secondary filtration through four layers of muslin interlaid with cotton wool. Thylakoids were then centrifuged (4000 × *g*) for 10 min and the pellet gently resuspended in washing medium (0.33 M sorbitol and 10 mM MED) before additional centrifugation. The pellet was then resuspended in resuspension medium (0.33 M sorbitol, 1 mM EDTA, 50 mM HEPES; pH 7.6) and osmotically shocked by mixing in 50 mL of break medium (10 mM HEPES; pH 7.6). After 30 s, osmotic potential was returned to normal with the addition of 50 mL of osmoticum

DOI: 10.1021/acs.jpclett.7b02634
J. Phys. Chem. Lett. XXXX, XXX, XXX–XXX

medium (0.66 M sorbitol, 40 mM MES; pH 6.5) and thylakoids centrifuged (4000 × *g*) for 10 min. The final pellet was resuspended in resuspension medium, and aliquots were frozen immediately in liquid nitrogen. The major LHCII complex was isolated from unstacked *Arabidopsis thaliana* thylakoids using isoelectric focusing.[37] The protein band corresponding to LHCII was collected and eluted in elution buffer containing 0.01% n-dodecyl *β*-D-maltoside (~200 *μ*M), then followed by size exclusion purification to remove ampholites (PD-10 columns, GE Healthcare). Aliquots of LHCII prepared at the same concentration (OD = 6) were immediately frozen in liquid nitrogen for later use in fluorescence analyses. While studying WT samples, we preferred not to use any additional artificial treatments of the isolated trimeric LHCII complexes, such as phospholipase, which is crucial for the monomerization of the trimers. Hence, we can compare the conformational dynamics in the naturally occurring WT LHCII trimers with that in the naturally occurring monomers of the mutant plants.

Streak Camera Measurements. Time-resolved fluorescence dynamics of the samples were measured by means of Hamamatsu C5680 streak camera with M5677 single-sweep module coupled to a spectrometer. Femtosecond Yb:KGW oscillator (Pharos, Light Conversion Ltd.) with a frequency doubler (HIRO, Light Conversion Ltd.) producing 515 nm sub-100 fs pulses at a 76 MHz repetition rate was employed, and a pulse picker was used to reduce the repetition rate to 20 kHz for nanosecond time scales. The beam was attenuated down to about 100 pJ per pulse and focused into about 100 *μ*m spot on the sample. No intensity dependence was observed when increasing the pulse energies by an order of magnitude or during the measurement process. The temporal resolution of the whole system was ~100 ps. All the measurements were performed at 273 K in a fused silica cell of 0.1 mm optical path. The obtained fluorescence decay kinetics, shown in Figure 1b, were independent of the detection wavelength (see Figure S2 for details).

Single-Molecule Microscopy Measurements. Buffer Solution: Buffer 1:10 mM Hepes (>99.5 Buffer grade, Carl-Roth Art.-Nr: HN07.1), 1 mM MgCl2 (>99 Cell pure, Carl-Roth Art.-Nr: HN78.2), 0.03% w/v Ÿ-DM (Lauryl-*β*-D-maltoside, > 99% for biochemistry, Art. CN26.2), pH = 7.8

Cleaning of Coverslips: Glass coverslips (Menzel-glaser #1.5) were placed in a staining jar and rinsed 3 times with ultrapure water (LaboStar, Siemens). Water was exchanged with 1% Alconox detergent solution (Alconox powdered precision cleaner) and the jar sonicated for 10 min (Ultrasonic Cleaning Unit RK 102H, Bandelin). Detergent solution was discarded from the jar and rinsed four times with ultrapure water. Water was exchanged with isopropanol (2-propanol ≥99.5%, art.no.:9866.6 Carl-Roth). Isopropanol was discarded, and the jar with coverslips was vacuumed in the plasma machine (PDC-002, Harric plasma) for 20 min, then plasma etched at ~400 mTorr pressure using maximal power for 5 min.

Surface Modification of Coverslips and Flow Cell Assembling: Clean glass coverslips were incubated with 0.01% of PLL (P4707 Sigma) for 10 min, then rinsed with Milli-Q, dried and assembled into the flow cell (sticky-slide VI 0.4, 80608, IBIDI) with the PLL modified side facing the sticky slide. Tubings were inserted into the inlet and outlet port of the cell and channel was filled with buffer1.

LHCII Immobilization and Imaging: 1.5e+05 diluted LHCII (2 *μ*g/mL) dissolved in buffer1 were injected into the flow cell channel and incubated for 3 min. 300 *μ*L of the buffer1 was injected to wash out the excess of unbound LHCII. For microscopy 100 *μ*L of buffer1 containing 15 units/ml glucose oxidase (from *Aspergillus niger*, G6125, Sigma-aldrich), 1% glucose (Ÿ-D-Glucose, G0047,TCI AMERICA). Measurements were performed at 23 °C.

SM TIRF Microscopy: The SM fluorescence microscopy setup used in this study was essentially the same as described previously except for a few important improvements.[38] All the dichroic mirrors in the setup were replaced with 2 mm thick TIRF flat parts glued in metal filter cubes (91032, Chroma). The 635 nm continuous-wave laser beam is expanded 66x. The laser beam was reflected off and the resulting fluorescence was transmitted through a zt532/635rps-XT (Chroma) dual-band dichroic mirror. The excitation light was filtered off by a quadruple-band interference filter FF01-446/510/581/703 (Semrock). The fluorescence image was split into two spectral components by T640lpxr-UF2 (Chroma) dichroic mirror. The 635 nm excitation intensity behind the objective was 0.6 mW and exposure time was 30 ms. In TIRF microscopy, light beam after passing the objective enters the sample with the high angle of incidence, so that at the interface of the regions with two different refractive indexes the evanescence field is generating, and technically it is difficult to measure its exact intensity.[39] However, according to our estimations, it should be far less than 1 W/cm^2, which corresponds to less than ~3 × 10^{18} photons per second per cm^2. Hence taking into account the mean absorption cross-section of the LHCII trimer, σ = 1.4 × 10^{-15} cm^2,[31] we conclude that the absorption rate should not exceed ~4500 photons per second per LHCII trimer.

In the EM-CCD camera used in this work, one detected photon corresponds to ~34 counts. The signal intensity (denoted in this work with a.u.) represents the amplitude of the 2D Gaussian fit, whose width was held constant and on average was equal to s = 1.33 pixels for all the detected spots. Therefore, one detected photon corresponds to the $34/(2\pi s^2)$ a.u. = 3 a.u.

Data Analysis: All data analysis procedures were performed and graphs prepared in Igor Pro (Wavemetrics) program using a custom written analysis package (available upon direct request to the author or under the link: http://www.igorexchange.com/project/TEA_MT). To detect immobilized LHCII, fluorescent spots were detected in images acquired using 635 nm laser. To make this detection more reliable, several frames from the beginning of the image series were averaged. From this averaged image a filtered image, enhancing the fluorescent spots, was generated and converted into a fluorescent spot probability image.[40] Spots having the probability above the manually defined value were fitted to the 2D symmetrical Gaussian to extract precise center position and width. Spots having higher than manually defined fitting error and center positions closer than 3 pixels were rejected. Intensity-versus-time dependency was extracted for all accepted spots from the series of images acquired at 635 nm excitation using 2D symmetrical Gaussian fit (center position and width was held constant). SM intensity was expressed by an amplitude of the 2D Gaussian fit. When LHCII switches into the dark state or bleaches out, the intensity of the local background becomes similar or sometimes even higher than in the center of the previously fluorescing spot. Therefore, sometimes intensity that we record becomes negative (i.e., the amplitude of the 2D Gaussian becomes less than 0). Hence in Figures 2−4, the 0 a.u. level can be treated as the mean intensity of the dark state. Finally, manual check and selection of those signals showing

DOI: 10.1021/acs.jpclett.7b02634
J. Phys. Chem. Lett. XXXX, XXX, XXX−XXX

characteristic single-molecule features (typical single-molecule fluorescence intensity and a single bleaching step) was performed. Only that selected data was used to make plots. SM fluorescence intensity traces were idealized using a custom-made intensity change point (ICP) detection algorithm without clustering. This algorithm is similar to a previously published method,[25] except that amplitude of the ICP is a constant and predefined by the user. Basically, it scans a trace point-by-point with an 8 point window, takes an average of the first 4 points and the last 4 points within the window and calculates a step amplitude (the difference between the averages) that is then compared with some threshold value. The latter was found empirically by testing different numerical values. Value of 40 a.u. for WT LHCII was high enough not to find any steps in the bleached part of the signal and low enough not to miss any significant steps in the active part of the signal. Next, we calculated step amplitude thresholds for mutant samples by multiplying the step amplitude of WT LHCII with a ratio between mean fluorescence intensity of WT and each of the mutant samples (Figure 2d). For example, for the *npq1lut2* and *aba4npq1lut2* mutants, 40/(125/110) = 35 a.u., and for *npq2lut2*, 40/(125/80) = 25 a.u. In the case where the step amplitude is higher than this threshold value, the center position of this window is recorded as a putative ICP. To be accepted, an ICP has to fulfill the criteria for the durations and slopes of the states it separates. Both states have to be not shorter than half of the scanning window length. The sum of the absolute slope values of the line fits of the states has to be smaller than a set value of 10.

■ ASSOCIATED CONTENT

Supporting Information

The Supporting Information is available free of charge on the ACS Publications website at DOI: 10.1021/acs.jpclett.7b02634.

Biexponential description of the fluorescence decay kinetics shown in Figure 1b, distributions of the fluorescence intensities at different time delays, demonstrating the bleaching of the observed single LHCII complexes, and fluorescence decay kinetics in various samples, detected at different wavelengths during the bulk streak camera measurements (PDF)

■ AUTHOR INFORMATION

Corresponding Author

*E-mail: leonas.valkunas@ff.vu.lt.

ORCID

Marijonas Tutkus: 0000-0002-5795-1347

Jevgenij Chmeliov: 0000-0002-7591-1373

Danielis Rutkauskas: 0000-0003-4705-2222

Notes

The authors declare no competing financial interest.

■ ACKNOWLEDGMENTS

We would like to acknowledge Dr. Petra Ungerer for providing the samples, Egidijus Songaila for the streak-camera fluorescence measurements, and Oskaras Venckus for help with the data analysis. J.C. and L.V. were supported by the Research Council of Lithuania (LMT Grant No. MIP-080/2015). A.R. was supported by The Royal Society Wolfson Research Merit Award and U.K. BBSRC Grant BB/L019027/1.

■ REFERENCES

(1) van Amerongen, H.; Valkunas, L.; van Grondelle, R. *Photosynthetic Excitons*; World Scientific: Singapore, 2000; p 590.

(2) Blankenship, R. E. *Molecular Mechanisms of Photosynthesis*, 2nd ed.; Wiley Blackwell: Chichester, U.K., 2014; p 296 p.

(3) Fleming, G. R.; Schlau-Cohen, G. S.; Amarnath, K.; Zaks, J. Design Principles of Photosynthetic Light-Harvesting. *Faraday Discuss.* **2012**, *155*, 27−41.

(4) Croce, R.; van Amerongen, H. Natural Strategies for Photosynthetic Light Harvesting. *Nat. Chem. Biol.* **2014**, *10*, 492−501.

(5) Ruban, A. V.; Johnson, M. P.; Duffy, C. D. P. The Photoprotective Molecular Switch in the Photosystem II Antenna. *Biochim. Biophys. Acta, Bioenerg.* **2012**, *1817*, 167−181.

(6) Holt, N. E.; Zigmantas, D.; Valkunas, L.; Li, X. P.; Niyogi, K. K.; Fleming, G. R. Carotenoid Cation Formation and the Regulation of Photosynthetic Light Harvesting. *Science* **2005**, *307*, 433−436.

(7) Pascal, A. A.; Liu, Z. F.; Broess, K.; van Oort, B.; van Amerongen, H.; Wang, C.; Horton, P.; Robert, B.; Chang, W. R.; Ruban, A. Molecular Basis of Photoprotection and Control of Photosynthetic Light-Harvesting. *Nature* **2005**, *436*, 134−137.

(8) Ruban, A. V.; Berera, R.; Ilioaia, C.; van Stokkum, I. H. M.; Kennis, J. T. M.; Pascal, A. A.; van Amerongen, H.; Robert, B.; Horton, P.; van Grondelle, R. Identification of a Mechanism of Photoprotective Energy Dissipation in Higher Plants. *Nature* **2007**, *450*, 575−578.

(9) Ahn, T. K.; Avenson, T. J.; Ballottari, M.; Cheng, Y. C.; Niyogi, K. K.; Bassi, R.; Fleming, G. R. Architecture of a Charge-Transfer State Regulating Light Harvesting in a Plant Antenna Protein. *Science* **2008**, *320*, 794−797.

(10) Staleva, H.; Komenda, J.; Shukla, M. K.; Šlouf, V.; Kaňa, R.; Polívka, T.; Sobotka, R. Mechanism of Photoprotection in the Cyanobacterial Ancestor of Plant Antenna Proteins. *Nat. Chem. Biol.* **2015**, *11*, 287−291.

(11) Chmeliov, J.; Gelzinis, A.; Songaila, E.; Augulis, R.; Duffy, C. D. P.; Ruban, A. V.; Valkunas, L. The Nature of Self-Regulation in Photosynthetic Light-Harvesting Antenna. Nat. *Plants* **2016**, *2*, 16045.

(12) Allen, J. F. Protein Phosphorylation in Regulation of Photosynthesis. *Biochim. Biophys. Acta, Bioenerg.* **1992**, *1098*, 275−335.

(13) Belgio, E.; Kapitonova, E.; Chmeliov, J.; Duffy, C. D. P.; Ungerer, P.; Valkunas, L.; Ruban, A. V. Economic Photoprotection in Photosystem II That Retains a Complete Light-Harvesting System with Slow Energy Traps. *Nat. Commun.* **2014**, *5*, 4433.

(14) Liu, Z. F.; Yan, H. C.; Wang, K. B.; Kuang, T. Y.; Zhang, J. P.; Gui, L. L.; An, X. M.; Chang, W. R. Crystal Structure of Spinach Major Light-Harvesting Complex at 2.72 Å Resolution. *Nature* **2004**, *428*, 287−292.

(15) Bishop, N. I. The *β,ε*-Carotenoid, Lutein, is Specifically Required for the Formation of the Oligomeric Forms of the Light Harvesting Complex in the Green Alga,. *J. Photochem. Photobiol., B* **1996**, *36*, 279−283.

(16) Fuciman, M.; Enriquez, M. M.; Polívka, T.; Dall'Osto, L.; Bassi, R.; Frank, H. A. Role of Xanthophylls in Light Harvesting in Green Plants: A Spectroscopic Investigation of Mutant LHCII and Lhcb Pigment−Protein Complexes. *J. Phys. Chem. B* **2012**, *116*, 3834−3849.

(17) Niyogi, K. K.; Shih, C.; Chow, W. S.; Pogson, B. J.; DellaPenna, D.; Björkman, O. Photoprotection in a Zeaxanthin- and Lutein-Deficient Double Mutant of Arabidopsis. *Photosynth. Res.* **2001**, *67*, 139−145.

(18) Bode, S.; Quentmeier, C. C.; Liao, P.-N.; Hafi, N.; Barros, T.; Wilk, L.; Bittner, F.; Walla, P. J. On the Regulation of Photosynthesis by Excitonic Interactions between Carotenoids and Chlorophylls. *Proc. Natl. Acad. Sci. U. S. A.* **2009**, *106*, 12311−12316.

(19) Müller, M. G.; Lambrev, P.; Reus, M.; Wientjes, E.; Croce, R.; Holzwarth, A. R. Singlet Energy Dissipation in the Photosystem II Light-Harvesting Complex Does Not Involve Energy Transfer to Carotenoids. *ChemPhysChem* **2010**, *11*, 1289−1296.

(20) Ware, M. A.; Dall'Osto, L.; Ruban, A. V. An In Vivo Quantitative Comparison of Photoprotection in Arabidopsis Xanthophyll Mutants. *Front. Plant Sci.* **2016**, *7*, 841.

DOI: 10.1021/acs.jpclett.7b02634
J. Phys. Chem. Lett. XXXX, XXX, XXX−XXX

(21) Dall'Osto, L.; Cazzaniga, S.; Bressan, M.; Paleček, D.; Žídek, K.; Niyogi, K. K.; Fleming, G. R.; Zigmantas, D.; Bassi, R. Two Mechanisms for Dissipation of Excess Light in Monomeric and Trimeric Light-Harvesting Complexes. *Nat. Plants* **2017**, *3*, 17033.
(22) Tian, L.; Xu, P.; Chukhutsina, V. U.; Holzwarth, A. R.; Croce, R. Zeaxanthin-Dependent Nonphotochemical Quenching Does Not Occur in Photosystem I in the Higher Plant. *Proc. Natl. Acad. Sci. U. S. A.* **2017**, *114*, 4828−4832.
(23) Havaux, M.; Dall'Osto, L.; Cuiné, S.; Giuliano, G.; Bassi, R. The Effect of Zeaxanthin as the Only Xanthophyll on the Structure and Function of the Photosynthetic Apparatus in Arabidopsis thaliana. *J. Biol. Chem.* **2004**, *279*, 13878−13888.
(24) Tutkus, M.; Marciulionis, T.; Sasnauskas, G.; Rutkauskas, D. DNA-Endonuclease Complex Dynamics by Simultaneous FRET and Fluorophore Intensity in Evanescent Field. *Biophys. J.* **2017**, *112*, 850−858.
(25) Krüger, T. P. J.; Ilioaia, C.; van Grondelle, R. Fluorescence Intermittency from the Main Plant Light-Harvesting Complex: Resolving Shifts between Intensity Levels. *J. Phys. Chem. B* **2011**, *115*, 5071−5082.
(26) Krüger, T. P. J.; Ilioaia, C.; Valkunas, L.; van Grondelle, R. Fluorescence Intermittency from the Main Plant Light-Harvesting Complex: Sensitivity to the Local Environment. *J. Phys. Chem. B* **2011**, *115*, 5083−5095.
(27) Krüger, T. P. J.; Wientjes, E.; Croce, R.; van Grondelle, R. Conformational Switching Explains the Intrinsic Multifunctionality of Plant Light-Harvesting Complexes. *Proc. Natl. Acad. Sci. U. S. A.* **2011**, *108*, 13516−13521.
(28) Krüger, T. P. J.; Ilioaia, C.; Johnson, M. P.; Ruban, A. V.; Papagiannakis, E.; Horton, P.; van Grondelle, R. Controlled Disorder in Plant Light-Harvesting Complex II Explains Its Photoprotective Role. *Biophys. J.* **2012**, *102*, 2669−2676.
(29) Schlau-Cohen, G. S.; Yang, H.-Y.; Krüger, T. P. J.; Xu, P.; Gwizdala, M.; van Grondelle, R.; Croce, R.; Moerner, W. E. Single-Molecule Identification of Quenched and Unquenched States of LHCII. *J. Phys. Chem. Lett.* **2015**, *6*, 860−867.
(30) Kondo, T.; Pinnola, A.; Chen, W. J.; Dall'Osto, L.; Bassi, R.; Schlau-Cohen, G. S. Single-Molecule Spectroscopy of LHCSR1 Protein Dynamics Identifies Two Distinct States Responsible for Multi-Timescale Photosynthetic Photoprotection. *Nat. Chem.* **2017**, *9*, 772−778.
(31) Krüger, T. P. J.; Novoderezhkin, V. I.; Ilioaia, C.; van Grondelle, R. Fluorescence Spectral Dynamics of Single LHCII Trimers. *Biophys. J.* **2010**, *98*, 3093−3101.
(32) Gruber, J. M.; Chmeliov, J.; Krüger, T. P. J.; Valkunas, L.; van Grondelle, R. Singlet-Triplet Annihilation in Single LHCII Complexes. *Phys. Chem. Chem. Phys.* **2015**, *17*, 19844−19853.
(33) Gwizdala, M.; Berera, R.; Kirilovsky, D.; Van Grondelle, R.; Krüger, T. P. Controlling Light Harvesting with Light. *J. Am. Chem. Soc.* **2016**, *138*, 11616−11622.
(34) Ruban, A. V.; Young, A. J.; Horton, P. Dynamic Properties of the Minor Chlorophyll *a*/*b* Binding Proteins of Photosystem II, an *in vitro* Model for Photoprotective Energy Dissipation in the Photosynthetic Membrane of Green Plants. *Biochemistry* **1996**, *35*, 674−678.
(35) Balevičius, V.; Gelzinis, A.; Abramavicius, D.; Mančal, T.; Valkunas, L. Excitation Dynamics and Relaxation in a Molecular Heterodimer. *Chem. Phys.* **2012**, *404*, 94−102.
(36) Fox, K. F.; Balevičius, V.; Chmeliov, J.; Valkunas, L.; Ruban, A. V.; Duffy, C. D. P. The Carotenoid Pathway: What is Important for Excitation Quenching in Plant Antenna Complexes? *Phys. Chem. Chem. Phys.* **2017**, *19*, 22957−22968.
(37) Ruban, A. V.; Young, A. J.; Pascal, A. A.; Horton, P. The Effects of Illumination on the Xanthophyll Composition of the Photosystem II Light-Harvesting Complexes of Spinach Thylakoid Membranes. *Plant Physiol.* **1994**, *104*, 227−234.
(38) Rutkauskas, D.; Petkelyte, M.; Naujalis, P.; Sasnauskas, G.; Tamulaitis, G.; Zaremba, M.; Siksnys, V. Restriction Enzyme Ecl18kI-Induced DNA Looping Dynamics by Single-Molecule FRET. *J. Phys. Chem. B* **2014**, *118*, 8575−8582.
(39) Martin-Fernandez, M.; Tynan, C.; Webb, S. A 'Pocket Guide' To Total Internal Reflection Fluorescence. *J. Microsc.* **2013**, *252*, 16−22.
(40) Yang, L.; Parton, R.; Ball, G.; Qiu, Z.; Greenaway, A. H.; Davis, I.; Lu, W. An Adaptive Non-Local Means Filter for Denoising Live-Cell Images and Improving Particle Detection. *J. Struct. Biol.* **2010**, *172*, 233−243.

DOI: 10.1021/acs.jpclett.7b02634
J. Phys. Chem. Lett. XXXX, XXX, XXX−XXX